INTERNATIONAL JOURNAL FOR NUMERICAL METHODS IN ENGINEERING
Int. J. Numer. Meth. Engng 2003; **56**:165–184 (DOI: 10.1002/nme.551)

A general non-linear optimization algorithm for lower bound limit analysis

Kristian Krabbenhoft and Lars Damkilde*,†

Department of Civil Engineering, Technical University of Denmark, DK-2800 Lyngby, Denmark

SUMMARY

The non-linear programming problem associated with the discrete lower bound limit analysis problem is treated by means of an algorithm where the need to linearize the yield criteria is avoided. The algorithm is an interior point method and is completely general in the sense that no particular finite element discretization or yield criterion is required. As with interior point methods for linear programming the number of iterations is affected only little by the problem size.

Some practical implementation issues are discussed with reference to the special structure of the common lower bound load optimization problem, and finally the efficiency and accuracy of the method is demonstrated by means of examples of plate and slab structures obeying different non-linear yield criteria. Copyright © 2002 John Wiley & Sons, Ltd.

KEY WORDS: limit analysis; finite element method; lower bound method; non-linear programming

1. INTRODUCTION

Limit analysis has been used in civil and mechanical engineering practice for decades as a means of estimating the ultimate strength of structures. Originally, hand calculations were used, and numerous methods such as the yield line method, the strip method, and the slip line method were developed. The success of limit analysis rests for a large part on the ability of these methods to provide quite accurate results for problems with relatively complicated geometries and loading conditions.

With the development of the modern computer it has become possible to reformulate the hand calculation methods in terms of methods suited for large numerical computations. As with the hand calculation methods the numerical computations can be based on either the upper or the lower bound theorem of plasticity, and are carried out as optimizations. With the upper bound method the most critical collapse mechanism is sought, where as the lower bound method involves a search for an admissible stress distribution which maximizes the load carrying capacity.

*Correspondence to: Lars Damkilde, Department of Chemistry and Applied Engineering Science, Aalborg University Esbjerg, DK-6700, Denmark
†E-mail: ld@aue.auc.dk

Received 3 May 2001
Revised 3 January 2002
Accepted 28 January 2002

In the following, the lower bound method will be used as this method is believed to have several advantages over the upper bound method. One obvious advantage is that the computed collapse loads are always on the safe side which for most applications is a desirable feature. Furthermore, the lower bound method is easily generalized. This generalization comes about by adopting the well-known finite element concept. In contrast to most elastic finite element formulations the elements are stress based rather than displacement based. With the stresses as the variables a set of equilibrium conditions can be formulated. Additionally, a set of yield conditions are imposed, and the final optimization problem can then be written as the maximization of a scalar load parameter subject to equilibrium and yield conditions.

2. PROBLEM FORMULATION

With the lower bound method the aim is to find a stress distribution which maximizes the intensity of a predefined external load. The stress distribution must be statically admissible, i.e. all equilibrium equations and yield conditions must be fulfilled. For a discrete structure the equilibrium equations can be written in matrix notation as

$$\mathbf{E}\boldsymbol{\sigma} = \alpha\mathbf{R} + \mathbf{R}_c \tag{1}$$

Here, $\mathbf{E}$ is an equilibrium matrix of n columns and m rows, $\boldsymbol{\sigma}$ is a vector containing the n stress parameters, and the external load consists of a constant part $\mathbf{R}_c$ and a part $\mathbf{R}$ proportional to a scalar load parameter α. As in all finite element procedures the equilibrium matrix and the load vectors are assembled from local element contributions, see Reference [1].

To prevent violation of the yield criteria an additional set of restrictions must be included. These can be written as

$$f_j(\boldsymbol{\sigma}) \leqslant 0, \quad j = 1, 2, \ldots, p \tag{2}$$

These restrictions will for all but the simplest structures be of a non-linear nature, but can usually be linearized in a straightforward manner.

With these two sets of constraints, linear equilibrium equations and non-linear yield criteria inequalities, the lower bound load optimization problem can be written as

$$\begin{aligned} &\text{maximize} && \alpha \\ &\text{subject to} && \mathbf{E}\boldsymbol{\sigma} = \alpha\mathbf{R} + \mathbf{R}_c \\ &&& f_j(\boldsymbol{\sigma}) \leqslant 0, \quad j = 1, 2, \ldots, p \end{aligned} \tag{3}$$

The inequalities can be converted to equalities by addition of positively restricted slack variables:

$$\begin{aligned} &\text{maximize} && \alpha \\ &\text{subject to} && \mathbf{E}\boldsymbol{\sigma} = \alpha\mathbf{R} + \mathbf{R}_c \\ &&& f_j(\boldsymbol{\sigma}) + s_j = 0, \quad s_j \geqslant 0, \ j = 1, 2, \ldots, p \end{aligned} \tag{4}$$

This formulation, in the following called a dual problem, is useful with respect to the solution algorithm presented in Section 3.

2.1. Duality between upper and lower bound methods

The duality theory of linear programming has an analogy in the duality between the upper and lower bound methods. With a problem originally formulated as lower bound one can construct the primal problem which for the discrete problem can be interpreted as the upper bound load optimization problem. This is a long established fact, and has been utilized to extract the collapse mechanism from problems originally formulated as lower bound, see e.g. Reference [2]. In the present it is used in the formulation of the solution algorithm.

Problem (4) may be linearized by considering the first-order Taylor expansion of the non-linear yield criteria around points $\boldsymbol{\sigma}^*$ lying on the yield surface

$$\mathbf{f}(\boldsymbol{\sigma}) \simeq \mathbf{f}(\boldsymbol{\sigma}^*) + \nabla \mathbf{f}^{\mathrm{T}}(\boldsymbol{\sigma} - \boldsymbol{\sigma}^*) \tag{5}$$

Since $\mathbf{f}(\boldsymbol{\sigma}^*) = \mathbf{0}$ the linearized yield conditions are

$$\nabla \mathbf{f}^{\mathrm{T}}\boldsymbol{\sigma} + \mathbf{s} = \nabla \mathbf{f}^{\mathrm{T}}\boldsymbol{\sigma}^* \tag{6}$$

The linearized lower bound problem then reads

$$\begin{aligned} &\text{maximize} && \alpha \\ &\text{subject to} && \mathbf{E}\boldsymbol{\sigma} = \alpha\mathbf{R} + \mathbf{R}_c \\ &&& \nabla \mathbf{f}^{\mathrm{T}}\boldsymbol{\sigma} + \mathbf{s} = \nabla \mathbf{f}^{\mathrm{T}}\boldsymbol{\sigma}^* \\ &&& \mathbf{s} \geqslant \mathbf{0} \end{aligned} \tag{7}$$

This is the form in which the lower bound load optimization problem with linearized yield conditions is usually cast. The dual to this problem is given by

$$\begin{aligned} &\text{minimize} && (\nabla \mathbf{f}^{\mathrm{T}}\boldsymbol{\sigma}^*)^{\mathrm{T}}\boldsymbol{\lambda} - \mathbf{R}_c^{\mathrm{T}}\mathbf{v} \\ &\text{subject to} && \nabla \mathbf{f}\boldsymbol{\lambda} - \mathbf{E}^{\mathrm{T}}\mathbf{v} = \mathbf{0} \\ &&& \mathbf{R}^{\mathrm{T}}\mathbf{v} = 1 \\ &&& \boldsymbol{\lambda} \geqslant \mathbf{0} \end{aligned} \tag{8}$$

Here $\boldsymbol{\lambda}$ contains the magnitude of each plastic strain, or strain rate, in accordance with the normality rule

$$\varepsilon_{ij}^{\mathrm{p}} = \lambda \frac{\partial f}{\partial \sigma_{ij}} \tag{9}$$

and $\mathbf{v}$ are the displacements, or velocities, at collapse. For the discrete problem this corresponds to the upper bound formulation of the load optimization problem. The expressions for the internal and external work rates are given by

$$W^{\mathrm{e}} = (\alpha\mathbf{R}^{\mathrm{T}} + \mathbf{R}_c^{\mathrm{T}})\mathbf{v}, \quad W^{\mathrm{i}} = (\nabla \mathbf{f}^{\mathrm{T}}\boldsymbol{\sigma}^*)^{\mathrm{T}}\boldsymbol{\lambda} \tag{10}$$

where α is the collapse load factor to be found as

$$\alpha = \min_{\mathbf{v},\boldsymbol{\lambda}} \left(\frac{(\nabla \mathbf{f}^{\mathrm{T}} \boldsymbol{\sigma}^*)^{\mathrm{T}} \boldsymbol{\lambda} - \mathbf{R}_c^{\mathrm{T}} \mathbf{v}}{\mathbf{R}^{\mathrm{T}} \mathbf{v}} \right) \tag{11}$$

With the external work fixed at 1 this reduces to the quantity minimized in problem (8).

In general the conditions

$$\nabla \mathbf{f} \boldsymbol{\lambda} - \mathbf{E}^{\mathrm{T}} \mathbf{v} = \mathbf{0} \tag{12}$$

can be interpreted as the conditions of compatibility between the plastic strains $\nabla \mathbf{f} \boldsymbol{\lambda}$ and the displacements $\mathbf{v}$. However, depending on the finite element discretization the elements in the displacement vector may have different interpretations. Using the so-called mixed finite element formulation the components of the displacement vector have a clear interpretation, namely as the displacements in the nodes of the assembled mesh, see e.g. Reference [2] or Reference [3]. However, in this work rigorous equilibrium elements are used. With these elements stress discontinuities are permitted provided that the normal and tangential stresses are continuous across element interfaces. The dual to this formulation of the lower bound method is the upper bound method with kinematically admissible velocity discontinuities, see Reference [4]. Whereas the mixed finite element formulation makes explicit reference to the stresses and displacements in each node of the assembled mesh, the equilibrium equations for the rigorous lower bound elements consist of a number of inter-element conditions securing static admissibility of the discontinuities and a number of overall equilibrium conditions. This is reflected in the displacement vector and must be taken into consideration when construction the displacement field, see Section 2.3.

2.2. *Optimality conditions*

In the following, the optimality conditions for the lower bound load optimization problem are derived and their physical interpretation is discussed. The conditions are derived by exploiting the duality between the upper and lower bound methods. The solution algorithm presented in Section 3 will be shown to be equivalent to solving these conditions iteratively.

From a mechanical point of view the solution to a limit analysis is achieved if there exists a kinematically admissible displacement field as well as a statically admissible stress field which, when the upper and lower bound theorems are applied give identical values of the collapse load. For the linearized lower bound problem (7) the conditions of static admissibility (dual feasibility) are

$$\mathbf{E}\boldsymbol{\sigma} = \alpha \mathbf{R} + \mathbf{R}_c \tag{13}$$

$$\nabla \mathbf{f}^{\mathrm{T}} \boldsymbol{\sigma} + \mathbf{s} = \nabla \mathbf{f}^{\mathrm{T}} \boldsymbol{\sigma}^* \tag{14}$$

$$\mathbf{s} \geqslant \mathbf{0} \tag{15}$$

whereas the primal feasibility conditions follow from (8) as

$$\nabla \mathbf{f} \boldsymbol{\lambda} - \mathbf{E}^{\mathrm{T}} \mathbf{v} = \mathbf{0} \tag{16}$$

$$\mathbf{R}^{\mathrm{T}}\mathbf{v} = 1 \tag{17}$$

$$\boldsymbol{\lambda} \geqslant \mathbf{0} \tag{18}$$

The condition that the primal and dual solutions be identical is expressed in terms of the duality gap γ, i.e. the gap between the primal and dual solutions, as

$$\gamma = (\nabla \mathbf{f}\boldsymbol{\sigma}^*)^{\mathrm{T}}\boldsymbol{\lambda} - \mathbf{R}_c^{\mathrm{T}}\mathbf{v} - \alpha = 0 \tag{19}$$

By using the feasibility conditions expressed in problems (7) and (8) the zero duality gap condition (19) can be written as

$$\begin{aligned}\gamma &= (\nabla \mathbf{f}^{\mathrm{T}}\boldsymbol{\sigma} + \mathbf{s})^{\mathrm{T}}\boldsymbol{\lambda} - (\mathbf{E}\boldsymbol{\sigma} - \alpha\mathbf{R})^{\mathrm{T}}\mathbf{v} - \alpha \\ &= \mathbf{s}^{\mathrm{T}}\boldsymbol{\lambda} + \boldsymbol{\sigma}^{\mathrm{T}}(\nabla \mathbf{f}\boldsymbol{\lambda} - \mathbf{E}^{\mathrm{T}}\mathbf{v}) + \alpha(\mathbf{R}^{\mathrm{T}}\mathbf{v} - 1) \\ &= \mathbf{s}^{\mathrm{T}}\boldsymbol{\lambda}\end{aligned} \tag{20}$$

Since both $\mathbf{s}$ and $\boldsymbol{\lambda}$ must be greater than or equal to zero condition (20) can be formulated as

$$s_j\lambda_j = 0, \quad j = 1, 2, \ldots, p \tag{21}$$

which is the condition of complementary slackness. In matrix notation it can be written as

$$\mathbf{S}\boldsymbol{\lambda} = \mathbf{0} \tag{22}$$

where $\mathbf{S} = \mathrm{diag}(\mathbf{s})$.

In applying the duality theory of linear programming the yield conditions were linearized as

$$\nabla \mathbf{f}^{\mathrm{T}}\boldsymbol{\sigma} + \mathbf{s} = \nabla \mathbf{f}^{\mathrm{T}}\boldsymbol{\sigma}^* \tag{23}$$

where $\mathbf{f}(\boldsymbol{\sigma}^*) = \mathbf{0}$. In order to be on the safe side an infinite number of such linear planes are needed which in the limit corresponds to the actual non-linear yield conditions

$$\mathbf{f}(\boldsymbol{\sigma}) + \mathbf{s} = \mathbf{0} \tag{24}$$

Thus, the linearized yield conditions can be substituted with the original ones and the full set of optimality conditions is then

$$\mathbf{E}\boldsymbol{\sigma} = \alpha\mathbf{R} + \mathbf{R}_c \tag{25}$$

$$\mathbf{f}(\boldsymbol{\sigma}) + \mathbf{s} = \mathbf{0} \tag{26}$$

$$\nabla \mathbf{f}\boldsymbol{\lambda} - \mathbf{E}^{\mathrm{T}}\mathbf{v} = \mathbf{0} \tag{27}$$

$$\mathbf{R}^{\mathrm{T}}\mathbf{v} = 1 \tag{28}$$

$$\mathbf{S}\boldsymbol{\lambda} = \mathbf{0} \tag{29}$$

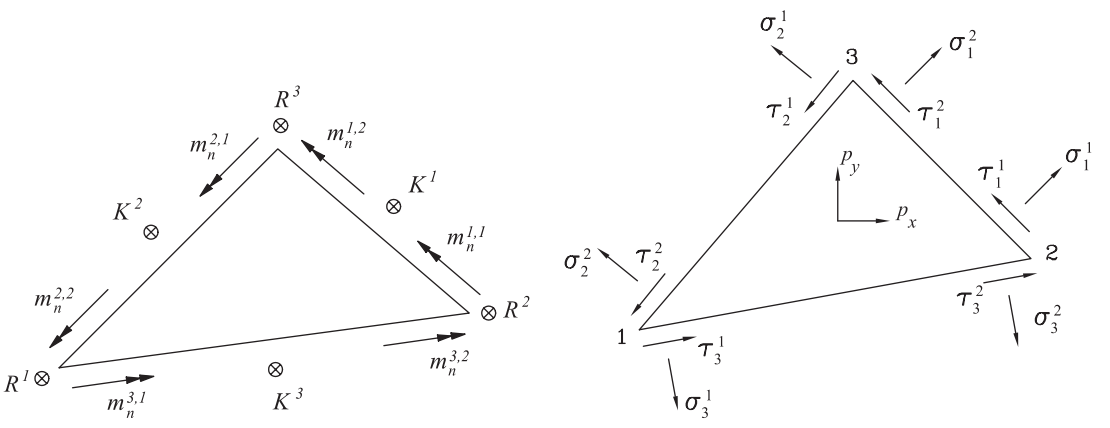

Figure 1. Plate elements for: (a) lateral loading; and (b) in-plane loading.

which are supplemented with the non-negativity requirements on $\mathbf{s}$ and $\boldsymbol{\lambda}$. In mathematical programming terms these are in fact the first-order Kuhn–Tucker optimality conditions, see e.g. Reference [5].

Thus, the optimality conditions include the feasibility requirements of the upper and lower bound formulations as given by (25)–(28). The variables appearing in the two formulations are connected through the condition that the duality gap should vanish (29). Apart from being the difference between the primal and dual solutions the duality gap establishes the necessary relation between the stresses and the strain rates. Associated with each yield condition check point in the finite element model is a slack variable s_j and a plastic strain rate λ_j. At the instant of collapse the strain rate λ_j may be zero in which case the stresses correspond to a point lying inside or on the yield surface, i.e. $s_j \geqslant 0$. Conversely, plastic flow may occur in which case $\lambda_j > 0$ and $s_j = 0$ since the stress point lies on the yield surface. In both situations the result is that $s_j \lambda_j = 0$.

2.3. *Finite element discretization*

The present solution algorithm does not require any particular formulations of the equilibrium equations, and as such any stress based finite element discretization is applicable. Thus, the generality of the lower bound method is not compromised by the optimization procedure. This is also the case with regard to the yield criteria where in principle any convex yield surface can be used.

In the present paper, the generality and efficiency of the method will be demonstrated be means of examples from slab and plate analysis with the yield criteria being those of Johansen, Coulomb, and von Mises.

The elements used are shown in Figure 1. In both the case of lateral and in-plane loading the variation of the moments and stresses, respectively, is linear. The variables, nine per element, are unique to each element and not to the nodes in the assembled mesh. The discontinuities in the variables at a corner where a number of elements are joined are countered by requiring continuity in the normal and tangential stresses across element boundaries. In

the plate bending element Kirchhoff boundary conditions have been imposed so that statically admissible discontinuities in the torsion moments across element interfaces are possible. With both elements the equilibrium equations are satisfied exactly. For the case of in-plane loading the equilibrium equations are given by

$$\frac{\partial \sigma_x}{\partial x} + \frac{\partial \tau_{xy}}{\partial y} + p_x = 0 \tag{30}$$

$$\frac{\partial \sigma_y}{\partial y} + \frac{\partial \tau_{xy}}{\partial x} + p_y = 0 \tag{31}$$

where p_x and p_y are body forces acting in the x and y directions, respectively. With constant body forces and linear stress fields within each element these equations can be satisfied exactly. Thus, the total equilibrium system consists of a number of inter-element equilibrium conditions and of conditions (30)–(31). When constructing the displacement field from the primal variables it is the variables associated with (30)–(31) which are used.

For a more detailed description of the elements we refer to Krabbenhoft and Damkilde [6] and Poulsen and Damkilde [7].

3. SOLUTION ALGORITHM

In recent years the limit analysis problem has been treated with algorithms where the need to linearize the yield constraints is avoided. In Reference [8] plane strain problems arising from a mixed finite element formulation are solved using a non-linear optimization method. This method is further developed by Lyamin [9] and Lyamin and Sloan [4] to deal with soil problems using the lower and upper bound methods, respectively.

Another approach has been taken by Christiansen and Andersen [3] who formulate the discrete limit analysis problem as the minimization of a sum of norms. This method seems, however, to lack some generality as only problems with quadratic von Mises-type yield criteria can be handled.

The first aim of the present paper is to formulate a general non-linear algorithm. Unlike the above-mentioned it should not require a particular finite element discretization or yield criterion. Secondly, the algorithm must be as simple as possible, both conceptually as well as with regard to the practical programming, and finally it must have an efficiency which is comparable to or better than existing algorithms. In this context, an algorithm for which the number of iterations required is insensitive to the problem size is preferable.

These requirements, and especially the last, cause us to search for an algorithm within the family of interior point methods. In Reference [6] a linear version of such an algorithm was used to formulate a cutting-plane method which turned out to be quite efficient.

The algorithm presented in this paper is an interior point path-following method based on the logarithmic barrier function. The origin of these methods goes back to the 1950s, see e.g. Reference [10], and were later discovered to have a formal relationship with the modern interior point methods such as the celebrated method of Karmarkar. A discussion of the methods in a modern context as applied to linear programming is given in Reference [11]. The basic ideas, however, apply not only to linear programming, and in the above mentioned work

of Christiansen and Andersen [3] a similar method was used for the non-linear optimization problem of minimizing a sum of norms, see also Reference [12].

As for all optimization problems, linear as well as non-linear, the key to the solution of the limit analysis problem lies in the formulation of a suitable set of optimality conditions. These are derived by using the first-order Kuhn–Tucker conditions, and the resulting set of conditions is shown to be equivalent to what was obtained in Section 2.2.

3.1. The path-following method

For the sake of convenience, we will consider a problem with the following notation

$$\begin{aligned} &\text{maximize} && \mathbf{b}^{\mathrm{T}}\mathbf{y} \\ &\text{subject to} && \mathbf{A}\mathbf{y} = \mathbf{c} \\ & && \mathbf{f}(\mathbf{y}) + \mathbf{s} = \mathbf{0}, \quad \mathbf{s} \geqslant \mathbf{0} \end{aligned} \tag{32}$$

This problem is identical to the lower bound load optimization problem (4) with

$$\begin{aligned} \mathbf{y} &= [\boldsymbol{\sigma}\ \alpha]^{\mathrm{T}} \\ \mathbf{b} &= [\mathbf{0}\ 1]^{\mathrm{T}} \\ \mathbf{A} &= [\mathbf{E}\ -\ \mathbf{R}] \\ \mathbf{c} &= \mathbf{R}_c \end{aligned} \tag{33}$$

Problem (32) is now modified by adding a barrier term in form of a logarithmic function

$$\begin{aligned} &\text{maximize} && w = \mathbf{b}^{\mathrm{T}}\mathbf{y} + \mu^k \sum_{j=1}^{p} \log s_j \\ &\text{subject to} && \mathbf{A}\mathbf{y} = \mathbf{c} \\ & && \mathbf{f}(\mathbf{y}) + \mathbf{s} = \mathbf{0} \end{aligned} \tag{34}$$

where μ^k again is a barrier parameter which will decrease as the iterations progress and the optimum is approached.

With the addition of the barrier term a sequence of problems with each optimal solution being close to the initial point are solved. In each iteration the initial point of the current subproblem is the point found in the previous iteration. If the barrier parameter is not reduced too abruptly the distance between the iterates is controlled, and the chances of the procedure converging are good.

In Figure 2 this is illustrated by the contour lines of an objective function modified by a logarithmic barrier term for different values of μ^k (the original object function is shown by dashed). As seen, the location of the optimal values of the different modified objective functions vary in a controlled manner along what is known as the central path towards the optimum located in $(0, 0)$, and with the steepest descent direction given in the figure as $\mathbf{b}$ becoming more and more dominant as the barrier parameter is reduced. For linear programs theoretical bounds on the maximum number of iterations required can be derived provided that μ^k is reduced in a special way, see, for example, Reference [5]. However, in practice

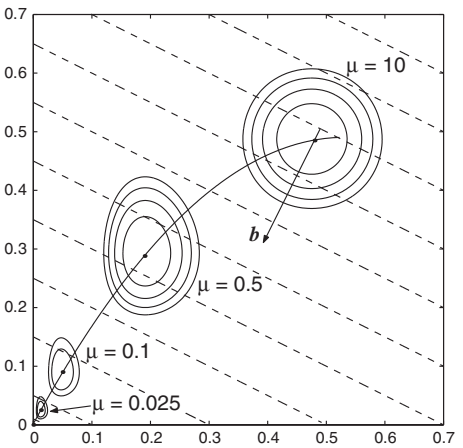

Figure 2. Convergence along the central path.

heuristic rules for reducing μ^k are usually applied and in most cases the algorithm performs much better than the theoretical bounds suggest.

The Kuhn–Tucker conditions can be used to derive the optimality conditions for the modified lower bound problem (34). The Lagrangian function is given by

$$\mathscr{L}(\mathbf{y},\mathbf{s},\boldsymbol{\lambda},\mathbf{v}) = \mathbf{b}^{\mathrm{T}}\mathbf{y} + \mu^k \sum_{j=1}^{p} \log s_j - \boldsymbol{\lambda}^{\mathrm{T}}(\mathbf{f}(\mathbf{y}) + \mathbf{s}) - \mathbf{v}^{\mathrm{T}}(\mathbf{c} - \mathbf{A}\mathbf{y}) \tag{35}$$

where the Lagrange multipliers have been denoted $\boldsymbol{\lambda}$ and $\mathbf{v}$.

The first-order Kuhn–Tucker optimality conditions require that the gradient of the Lagrangian vanishes, that is

$$\nabla\mathscr{L}(\mathbf{y},\mathbf{s},\boldsymbol{\lambda},\mathbf{v}) = \begin{bmatrix} \dfrac{\partial\mathscr{L}}{\partial\mathbf{y}} \\ \dfrac{\partial\mathscr{L}}{\partial\mathbf{s}} \\ \dfrac{\partial\mathscr{L}}{\partial\boldsymbol{\lambda}} \\ \dfrac{\partial\mathscr{L}}{\partial\mathbf{v}} \end{bmatrix} = \begin{bmatrix} \mathbf{0} \\ \mathbf{0} \\ \mathbf{0} \\ \mathbf{0} \end{bmatrix} \tag{36}$$

These conditions can be written as

$$\mathbf{r} = \begin{bmatrix} \mathbf{r}_1 \\ \mathbf{r}_2 \\ \mathbf{r}_3 \\ \mathbf{r}_4 \end{bmatrix} = \begin{bmatrix} \nabla_y\mathbf{f}(\mathbf{y})\boldsymbol{\lambda} - \mathbf{A}^{\mathrm{T}}\mathbf{v} - \mathbf{b} \\ \mathbf{S}\boldsymbol{\lambda} - \mu^k\mathbf{e} \\ \mathbf{f}(\mathbf{y}) + \mathbf{s} \\ \mathbf{c} - \mathbf{A}\mathbf{y} \end{bmatrix} = \begin{bmatrix} \mathbf{0} \\ \mathbf{0} \\ \mathbf{0} \\ \mathbf{0} \end{bmatrix} \tag{37}$$

where $\mathbf{e}$ is a vector of ones.

Table I. Algorithm.

Initial point $\mathbf{y}^0 = \mathbf{0}$, $\mathbf{v}^0 = \mathbf{0}$, $\mathbf{s}^0 = \mathbf{e}$, $\boldsymbol{\lambda}^0 = \mathbf{e}$
Barrier parameter $\mu^0 = 0.2(\mathbf{s}^0)^{\mathrm{T}}\boldsymbol{\lambda}^0/p$
Iterations $k = 1, \ldots, n$
Assemble $\mathbf{r}^{k-1}$ (37) and $\mathbf{T}^{k-1}$ (39)
Compute direction $\Delta\mathbf{p}$ by solving $\mathbf{T}^{k-1}\Delta\mathbf{p} = \mathbf{r}^{k-1}$
Update variables such that $\mathbf{s}^k > \mathbf{0}$ and $\boldsymbol{\lambda}^k > \mathbf{0}$
Update barrier parameter $\mu^k = 0.2(\mathbf{s}^k)^{\mathrm{T}}\boldsymbol{\lambda}^k/p$

In the limit of $\mu^k = 0$ these optimality conditions are seen to be identical to what was found in the previous section, with $\mathbf{r}_1 = \mathbf{0}$ corresponding to the upper bound feasibility conditions (27) and (28), $\mathbf{r}_2 = \mathbf{0}$ to the complementary slackness condition (29), $\mathbf{r}_3 = \mathbf{0}$ to the yield conditions (26), and $\mathbf{r}_4 = \mathbf{0}$ to the equilibrium conditions (25).

Newton's method may now be applied to the system of non-linear equations (37). With this method a direction $\Delta\mathbf{p} = (\Delta\mathbf{y},\ \Delta\mathbf{s},\ \Delta\boldsymbol{\lambda},\ \Delta\mathbf{v})$ is found by solution of the system

$$\mathbf{T}\Delta\mathbf{p} = -\mathbf{r} \tag{38}$$

where

$$\mathbf{T} = \nabla\mathbf{r} = \begin{bmatrix} \mathbf{H} & \mathbf{0} & \nabla_y\mathbf{f}(\mathbf{y}) & -\mathbf{A}^{\mathrm{T}} \\ \mathbf{0} & \boldsymbol{\Lambda} & \mathbf{S} & \mathbf{0} \\ \nabla_y\mathbf{f}(\mathbf{y})^{\mathrm{T}} & \mathbf{I} & \mathbf{0} & \mathbf{0} \\ -\mathbf{A} & \mathbf{0} & \mathbf{0} & \mathbf{0} \end{bmatrix} \tag{39}$$

Here $\boldsymbol{\Lambda} = \mathrm{diag}(\boldsymbol{\lambda})$, $\mathbf{I}$ is a unit matrix, and

$$\mathbf{H} = \sum_{j=1}^{n} \lambda_j \nabla^2_{yy} f_j(\mathbf{y}) \tag{40}$$

The algorithm proceeds by updating and solving equation (39) in each iteration. This gives a direction from which the new point can be computed. Also in each iteration a value of the barrier parameter must be chosen which is usually done by relating it to the value of the duality gap $\gamma = \mathbf{s}^{\mathrm{T}}\boldsymbol{\lambda}$. In the simplest form the algorithm consists of the steps shown in Table I where some typical values of the different parameters and initial values have been used.

Since the only requirement to the starting point of the algorithm is that $\mathbf{s}$ and $\boldsymbol{\lambda}$ are positive it is in practice these variables which determine the magnitude of the iteration steps. The variables are updated as

$$\begin{aligned} \mathbf{y}^k &= \mathbf{y}^{k-1} + \eta_D\Delta\mathbf{y}, \quad \mathbf{s}^k = \mathbf{s}^{k-1} + \eta_D\Delta\mathbf{s} \\ \boldsymbol{\lambda}^k &= \boldsymbol{\lambda}^{k-1} + \eta_P\Delta\boldsymbol{\lambda}, \quad \mathbf{v}^k = \mathbf{v}^{k-1} + \eta_P\Delta\mathbf{v} \end{aligned} \tag{41}$$

where superscript k counts iterations, and η_P and η_D are appropriate step lengths. These must be chosen such that $\mathbf{s}$ and $\boldsymbol{\lambda}$ remain positive. The maximum step lengths are determined by line search as

$$\eta_D^{\max} = \min_{\Delta \mathbf{s}_i < 0} (-\mathbf{s}_i^{k-1} / \Delta \mathbf{s}_i), \quad \eta_P^{\max} = \min_{\Delta \boldsymbol{\lambda}_i < 0} (-\boldsymbol{\lambda}_i^{k-1} / \Delta \boldsymbol{\lambda}_i) \tag{42}$$

For linear interior point methods practical experience has shown that the fastest convergence is achieved if the step lengths are chosen as being slightly smaller than the maximum permissible, i.e. if the step lengths are determined as

$$\eta_D = \theta \eta_D^{\max}, \quad \eta_P = \theta \eta_P^{\max} \tag{43}$$

where θ is close to 1. In our implementation a value of $\theta = 0.99$ has turned out to be a good compromise between the efficiency of the algorithm and the stability of the equation system.

At this point we should emphasize that the term 'interior point' refers to the interior of the feasible $\mathbf{s}$ and $\boldsymbol{\lambda}$ spaces and not to the interior of the yield locus as is the case with the methods of Lyamin [9] and Zouain *et al.* [8]. In fact the yield conditions may very well be violated in the course of the iterations, and the lower bound nature of the method thus depends on choosing a suitable convergence criterion for the yield conditions.

3.2. Implementation issues

In the following, some implementation issues are discussed with reference to the special structure of the common limit analysis problem.

3.2.1. Reduction of equation system. The highly sparse non-symmetric matrix $\mathbf{T}$ (39) has rank $n + m + 2p$. Thus, the number of yield constraints has a significant influence on the problem size. However, the size of the matrix to be factorized in each iteration can be made dependent on the number of equilibrium equations only. This is done by expressing $\Delta \mathbf{s}$ and $\Delta \boldsymbol{\lambda}$ as

$$\Delta \mathbf{s} = -(\mathbf{r}_3 + \nabla \mathbf{f}^{\mathrm{T}} \Delta \mathbf{y}), \quad \Delta \boldsymbol{\lambda} = -\mathbf{S}^{-1}(\mathbf{r}_2 + \boldsymbol{\Lambda} \Delta \mathbf{s}) \tag{44}$$

These expressions are inserted into (38) which then yields

$$\begin{bmatrix} -\mathbf{W} & \mathbf{A}^{\mathrm{T}} \\ \mathbf{A} & \mathbf{0} \end{bmatrix} \begin{bmatrix} \Delta \mathbf{y} \\ \Delta \mathbf{v} \end{bmatrix} = \begin{bmatrix} \mathbf{q} \\ \mathbf{r}_4 \end{bmatrix} \tag{45}$$

where

$$\begin{aligned} \mathbf{W} &= \mathbf{H} + \nabla \mathbf{f} \mathbf{S}^{-1} \boldsymbol{\Lambda} \nabla \mathbf{f}^{\mathrm{T}} \\ \mathbf{q} &= \mathbf{r}_1 + \nabla \mathbf{f} \mathbf{S}^{-1} (\boldsymbol{\Lambda} \mathbf{r}_3 - \mathbf{r}_2) \end{aligned} \tag{46}$$

If $\mathbf{W}$ is non-singular system (45) can be reduced further by first solving for $\Delta \mathbf{v}$

$$(\mathbf{A} \mathbf{W}^{-1} \mathbf{A}^{\mathrm{T}}) \Delta \mathbf{v} = \mathbf{r}_4 + \mathbf{A} \mathbf{W}^{-1} \mathbf{q} \tag{47}$$

and subsequently for $\Delta\mathbf{y}$

$$\Delta\mathbf{y} = \mathbf{W}^{-1}(\mathbf{A}^{\mathrm{T}}\Delta\mathbf{v} - \mathbf{q}) \tag{48}$$

However, for some yield criteria, e.g. the unbounded von Mises and Coulomb plane strain criteria, $\mathbf{W}$ will be singular. In Reference [3] this problem is overcome by elimination. Another way of dealing with the problem is to add a small number to the diagonal of $\mathbf{H}$

$$\mathbf{H} = \delta\mathbf{I} + \sum_{j=1}^{n} \lambda_j \nabla^2_{yy} f_j(\mathbf{y}) \tag{49}$$

where $\delta = 10^{-5}\max(\boldsymbol{\lambda})$ has been used successfully.

In summary, the computation of the increments follows a four step procedure with $\Delta\mathbf{v}$ being determined by (47), followed by the computation of $\Delta\mathbf{y}$ (48) and $\Delta\mathbf{s}$ and $\Delta\boldsymbol{\lambda}$ (44).

Since $\mathbf{W}$ is a block diagonal, for most yield criteria consisting of 3 by 3 blocks, inversion is very fast, and the speed-up obtained by using the four step procedure compared to solving (45) directly is roughly a factor of 10.

3.2.2. Predictor–corrector scheme. Mehrotra [13] has suggested a predictor–corrector method in connection with the solution of system (38). Although this method was applied to the case where all constraints are linear the general principle can still be applied in the non-linear case. The predictor–corrector method is concerned with the equation

$$\mathbf{S}\boldsymbol{\lambda} = \mu^k\mathbf{e} \tag{50}$$

With Newton's method this is solved iteratively with increments $\Delta\mathbf{s}$ and $\Delta\boldsymbol{\lambda}$ determined by

$$\mathbf{S}\boldsymbol{\lambda} + \boldsymbol{\Lambda}\Delta\mathbf{s} + \mathbf{S}\Delta\boldsymbol{\lambda} = \mu^k\mathbf{e} \tag{51}$$

whereas, if an exact solution was to be obtained the increments would have to satisfy

$$(\mathbf{S} + \Delta\mathbf{S})(\boldsymbol{\lambda} + \Delta\boldsymbol{\lambda}) = \mu^k\mathbf{e} \tag{52}$$

which differs from (51) only in the non-linear term $\Delta\mathbf{S}\Delta\boldsymbol{\lambda}$.

For an improved convergence Mehrotra suggested solving Equation (52) in two steps. In the first predictor step the non-linear term $\Delta\mathbf{S}\Delta\boldsymbol{\lambda}$ as well as the right-hand side are dropped. The predicted values of $\mathbf{s}$ and $\boldsymbol{\lambda}$ are then used to compute an estimate of $\Delta\mathbf{S}\Delta\boldsymbol{\lambda}$ and in turn a good value of μ^k. This is followed by the corrector step in which the predicted values are used to obtain improved estimates of the increments. The procedure is as shown in Table II. With respect to the barrier parameter a commonly used rule for linear programming is

$$\mu^k = \min\{1, (\hat{\mathbf{s}}^{\mathrm{T}}\hat{\boldsymbol{\lambda}}/p\mu^{k-1})^{\xi}\}\mu^{k-1} \tag{53}$$

where

$$\hat{\mathbf{s}} = \mathbf{s} + \Delta\hat{\mathbf{s}}, \quad \hat{\boldsymbol{\lambda}} = \boldsymbol{\lambda} + \Delta\hat{\boldsymbol{\lambda}} \tag{54}$$

This rule has turned out to work well with $\xi = 1.0 - 2.0$ and $\mu^0 = (\mathbf{s}^0)^{\mathrm{T}}\boldsymbol{\lambda}^0/p$.

Table II. Algorithm.

Initial point $\mathbf{y}^0$, $\mathbf{v}^0$, $\mathbf{s}^0$, $\boldsymbol{\lambda}^0$ and barrier parameter μ^0
Iterations $k = 0, 1, \ldots, n$
Predictor step, $\mathbf{r}_2 = \mathbf{S}\boldsymbol{\lambda}$
Compute directions according to (47), (48), (44)
Determine maximum increments $\Delta\hat{\mathbf{s}}, \Delta\hat{\boldsymbol{\lambda}}$
Compute barrier parameter μ^k
Corrector step, $\mathbf{r}_2 = \mathbf{S}\boldsymbol{\lambda} + \Delta\hat{\mathbf{S}}\Delta\hat{\boldsymbol{\lambda}} - \mu^k\mathbf{e}$
Compute directions according to (47), (48), (44)
Update variables according to (41)

3.2.3. Dense columns. In maintaining sparsity of the product $\mathbf{A}\mathbf{W}^{-1}\mathbf{A}^{\mathrm{T}}$ it is essential that $\mathbf{A} = [\mathbf{E} - \mathbf{R}]$ does not contain any dense columns. However, as many problems will often contain a large number of load components, e.g. problems of plates and slabs subjected to distributed loads, $\mathbf{A}\mathbf{W}^{-1}\mathbf{A}^{\mathrm{T}}$ will usually be rather dense if no special provision are taken.

There is a number of ways of dealing with dense columns, most of them based on a Cholesky factorization of $\mathbf{A}\mathbf{W}^{-1}\mathbf{A}^{\mathrm{T}}$. These methods require the that product to be factorized is positive definite which in the general case may not be fulfilled. Therefore, in the present a different approach to maintaining sparsity is taken, namely by splitting up the dense column $\mathbf{R}$. We modify the original matrix $\mathbf{A}$ as

$$\mathbf{A} = [\mathbf{E} - \mathrm{diag}(\mathbf{R}_{nz})] \tag{55}$$

where $\mathrm{diag}(\mathbf{R}_{nz})$ is equal to $\mathrm{diag}(\mathbf{R})$ with zero columns deleted.

This corresponds to extending the single load parameter α to a vector of load parameters $\boldsymbol{\alpha} = [\alpha_1, \alpha_2, \ldots, \alpha_l]^{\mathrm{T}}$ such that each non-zero load component is optimized independently. To secure proportional loading an additional number of constraints is necessary, and the equilibrium and load constraints can then be written as

$$\mathbf{A}'\mathbf{y}' = \mathbf{c}' \tag{56}$$

where

$$\mathbf{A}' = \begin{bmatrix} \mathbf{E} & -\mathrm{diag}(\mathbf{R}_{nz}) \\ \mathbf{0} & \mathbf{G} \end{bmatrix}, \quad \mathbf{y}' = \begin{bmatrix} \boldsymbol{\sigma} \\ \boldsymbol{\alpha} \end{bmatrix}, \quad \mathbf{c}' = \begin{bmatrix} \mathbf{R}_c \\ \mathbf{0} \end{bmatrix} \tag{57}$$

and the constraints $\mathbf{G}\boldsymbol{\alpha} = \mathbf{0}$ are of the type

$$\begin{aligned} \alpha_1 - \alpha_2 &= 0 \\ \alpha_2 - \alpha_3 &= 0 \\ &\ddots \\ \alpha_{l-1} - \alpha_l &= 0 \end{aligned} \tag{58}$$

under the assumption that the number of non-zero load components l is greater than 1.

3.2.4. Other issues. Other important issues such as the choice of the initial point, other rules for updating the barrier parameter, the choice of the barrier proximity parameter, whether or not to use a common step length $\eta = \min(\eta_P, \eta_D)$, and the possibility of multiple corrector steps, fall outside the scope of this paper, and we instead refer to References [5, 11, 13].

4. EXAMPLES

In this section, three examples demonstrating the capabilities of the proposed method are given. Both examples of laterally loaded plates as well as plates subjected to in-plane forces are given, and the yield criteria considered are those of von Mises, Johansen, and Coulomb.

For all examples the iterations are broken off when the following criteria are fulfilled

$$\max(\mathbf{f}(\boldsymbol{\sigma})) < 10^{-5}, \quad \|\mathbf{E}\boldsymbol{\sigma} - \alpha\mathbf{R}\| < 10^{-10} \tag{59}$$

The duality gap at the point where the iterations are broken off gap varies quite significantly depending on the yield criterion used, with the Johansen criterion being the most sensitive. However, as we are concerned with lower bound limit analysis the two above conditions on the yield criteria and the equilibrium equations have been deemed satisfactory.

All implementation was done in Matlab 5.3, and the examples run on a 400 MHz desktop PC.

4.1. Slotted block in plane strain

The following example is taken from Andersen and Christiansen [3]. A square block of material with two slots machined in it as shown in Figure 3(a) is considered. The strength of the material is governed by the von Mises yield criterion, and the state of deformation is plane, i.e. the yield criterion reads

$$\tfrac{1}{4}(\sigma_x - \sigma_y)^2 + \tau_{xy}^2 = \tfrac{1}{3}\sigma_0^2 \tag{60}$$

As in Reference [3] we have set $\sigma_0 = \sqrt{3}$. The mesh used is shown in Figure 3(b). The fact that the shear stresses vanish along the lines of symmetry is utilized such that only one quarter of the block is modelled.

The results obtained with various element meshes are shown in Table III. The results are very satisfactory with even very moderate meshes giving results with errors which for all practical purposes are negligible. A comparison between the element used in the present paper and the mixed formulation used in Reference [3] is shown in Figure 4. The present

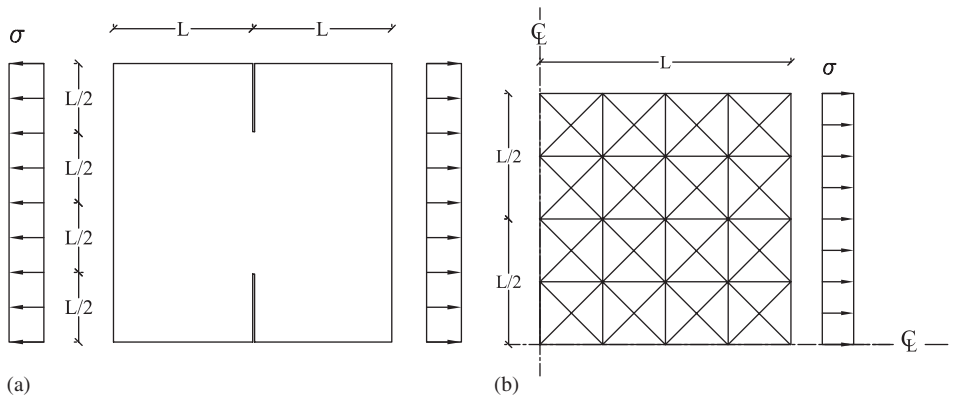

Figure 3. (a) Slotted block problem; and (b) element discretization, $N = 4$.

Table III. Solution statistics, von Mises plane strain example.

N	Vars.	Equil.	Yield	σ_c	Err.† (%)	Iter.	Time (ms)
2	148	137	48	1.11404	1.55	9	0:01
4	584	523	192	1.12703	0.40	11	0:06
8	2320	2039	768	1.13050	0.09	13	0:28
12	5208	4547	1728	1.13108	0.042	15	1:56
16	9248	8047	3072	1.13128	0.025	16	4:40
20	14440	12539	4000	1.13138	0.016	17	8:55
24	20784	18023	6912	1.13143	0.011	17	18:40
30	32460	28109	10800	1.13148	0.0075	18	40:18
34	41684	36073	13872	1.13149	0.0060	19	72:32
38	52060	45029	17328	1.13150	0.0052	20	110:42

† With respect to extrapolated value $\sigma_c = 1.13156$ from Reference [3].

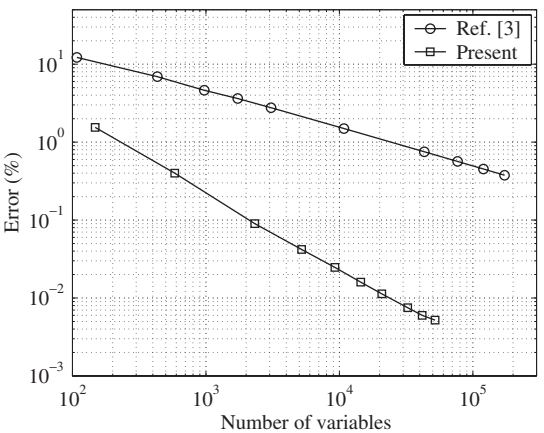

Figure 4. Slotted block problem. Results with different elements.

element appears to be vastly superior to the mixed formulation. For $N = 4$ corresponding to 584 stress and load parameter variables the error is similar to what is obtained in Reference [3] with the use of approximately 170 000 stress variables. A more detailed analysis shows that whereas the error in Reference [3] is $O(1/N)$ the present results show an error of $O(1/N^2)$. Furthermore, whereas the results obtained with the present element are always lower bounds, the mixed formulation does not bound the true collapse load in any consistent way and the results may thus, depending on the example, be either upper or lower bounds.

As for the optimization algorithm the number of iterations increases only very slowly with the problem size as is generally the case with interior point methods for linear programming.

The velocity field is shown in Figure 5. As seen the velocities taken at the centre of each element define a slip line field consisting of two distinct discontinuities as indicated in the figure—one from the cut to a point near the right edge consisting of a logarithmic spiral, which in the case of zero friction reduces to a circular arc, and one extending from this point and outwards perpendicular to the first slip line.

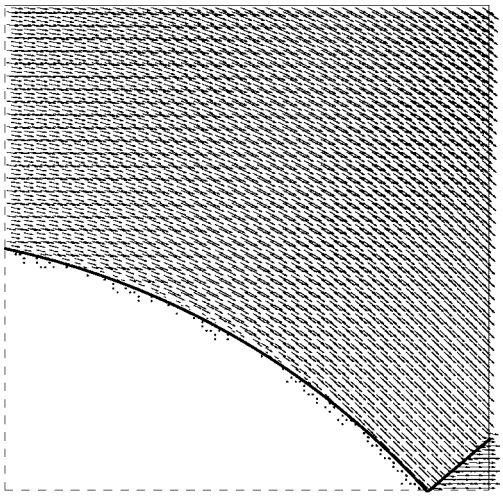

Figure 5. Slip lines and velocities.

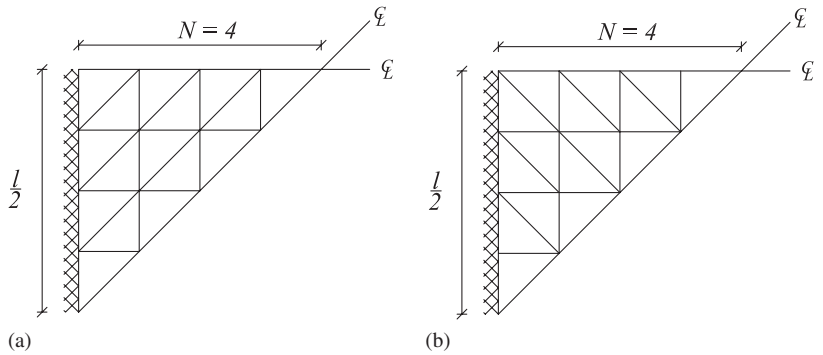

Figure 6. Element meshes (a) and (b).

4.2. *Clamped square concrete plate subjected to uniform pressure*

A common test example for plate bending elements is that of a clamped square plate subjected to a uniformly distributed load.

In the following, the symmetry of the problem is utilized and one-eighth of the plate modelled. Two different meshes (a) and (b), shown if Figure 6, are considered. The material obeys Johansen's yield criterion

$$\begin{aligned} -(m_\mathrm{p} - m_x)(m_\mathrm{p} - m_y) + m_{xy}^2 &\leqslant 0 \\ -(m_\mathrm{p} + m_x)(m_\mathrm{p} + m_y) + m_{xy}^2 &\leqslant 0 \\ -m_\mathrm{p} \leqslant m_x &\leqslant m_\mathrm{p} \\ -m_\mathrm{p} \leqslant m_y &\leqslant m_\mathrm{p} \end{aligned} \tag{61}$$

where m_p is the yield moment. This criterion is commonly used for reinforced concrete. For a plate of a material obeying Johansen's yield criterion the exact value of the collapse load

Table IV. Collapse loads pl^2/m_p for square clamped plate for meshes (a) left and (b) right.

N	p_a	Err. (%)	Iter.	p_b	Err. (%)	Iter.
2	40.696	5.02	14	40.923	4.50	12
4	42.156	1.62	15	42.023	1.93	14
6	42.452	0.93	14	42.333	1.21	14
8	42.566	0.67	14	42.520	0.77	14
12	42.681	0.40	16	42.663	0.44	19
20	42.755	0.22	18	42.755	0.22	19
30	42.789	0.14	21	42.793	0.14	20
40	42.802	0.11	20	42.806	0.11	21
50	42.816	0.081	21	42.820	0.073	20

Table V. Comparison between collapse loads for meshes (a) left and (b) right.

N	p_a/p_a (Reference [2])	p_b/p_b (Reference [2])
2	1.036	0.974
4	1.023	1.007
6	1.027	1.037
8	1.035	1.030

was found by Fox [14] as

$$p_e = 42.851 \frac{m_p}{l^2} \tag{62}$$

with l being the length of the plate.

The numerically obtained results are given in Table IV. As seen, useful results are obtained with a moderate number of elements, and for the finest mesh used (2500 elements resulting in 22 500 moment variables) the error is less than 0.1%. Furthermore, the element appears to be quite insensitive to the orientation of the diagonals in the mesh.

The iteration counts are similar to those of the previous example, and this in spite of the fact that the Johansen yield criterion is much more complicated geometrically than the von Mises criterion.

In Reference [2] the example has also been examined. Here the non-linear yield surface was approximated by eight linear planes and the equilibrium equations were set up using a mixed finite element formulation. A comparison between the results given in Reference [2] and the results obtained with the present element and optimization method is given in Table V. As can be seen from the table the present collapse loads are approximately 2–4% higher than the results obtained in Reference [2], which is typically what can be gained by using the full non-linear representation of the yield criterion rather than the eight hyper plane linearization. For mesh (b) the collapse load found in Reference [2] is seen to greater than what is found with the equilibrium elements used in this work. This is due to the mixed finite element discretization in Reference [2] which permits local equilibrium violations.

The displacements are shown in Figure 7 for mesh (a) and different values of the mesh size parameter N. The displacements seem to vanish in the corners indicating rigid parts which is in agreement with Fox' solution. Already for $N = 2$ which is a quite coarse mesh, the collapse field has some of the characteristics of the exact field. For $N = 4$ the error is still smaller,

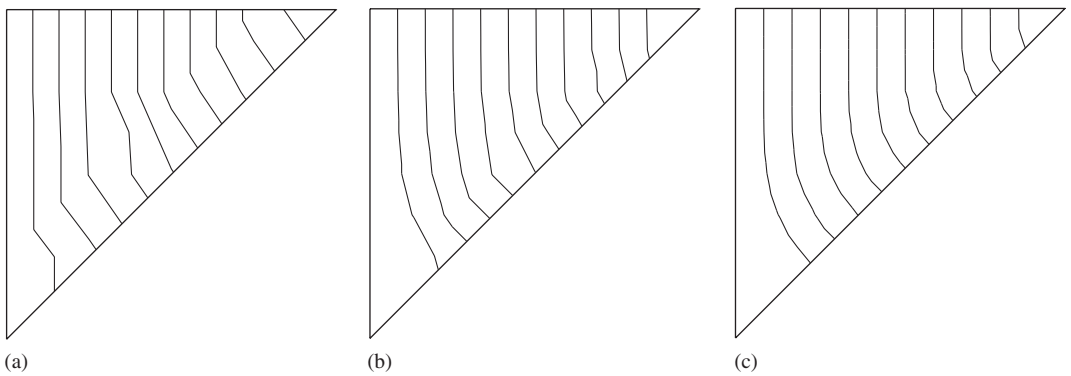

Figure 7. Lines of constant displacement: (a) $N = 2$; (b) $N = 4$; and (c) $N = 8$.

and from $N = 8$ the displacement solution does not improve significantly, i.e. a convergence rate similar to that of the collapse load can be observed.

4.3. Expansion of cohesive-frictional cylinder

In the following, a problem governed by the Coulomb yield criterion is considered. Under plane strain assumptions the yield criterion can be expressed as

$$(\sigma_x - \sigma_y)^2 + 4\tau_{xy}^2 - (2c\cos\phi - (\sigma_x + \sigma_y)\sin\phi)^2 = 0 \tag{63}$$

where c is the cohesion and ϕ is the angle of friction. The exact solution for a weightless cylinder of a cohesive-frictional material subjected to internal pressure has been obtained by Yu [15] as

$$p = \frac{2c\cos\phi}{(\alpha - 1)(1 - \sin\phi)} \left(\left(\frac{b}{a} \right)^{(\alpha-1)/\alpha} - 1 \right) \tag{64}$$

where p is the collapse pressure, a and b are the inner and outer radii, respectively, and $\alpha = \tan^2(45^\circ + \phi/2)$. In the limit of $\phi = 0$, i.e. $\alpha = 1$ the collapse pressure reduces to

$$p = 2c\ln\frac{b}{a} \tag{65}$$

In the following $b/a = 2$, $c = 1.0$, and $\phi = 30^\circ$ which gives a value of the exact collapse pressure as $p_e = 1.0174$. By utilizing the symmetry only a 90° sector of the cylinder is modelled as shown in Figure 8.

Three different meshes were used and the collapse pressures determined as shown in Table VI.

As with the previous examples the number of iterations increases only slowly as the problem size increases. The deviation of the computed results from the exact solution, for the finest mesh just 0.61%, is also satisfactory.

In Figure 9 the velocity field corresponding the finest mesh is shown. As expected the velocities correspond to a collapse mechanism with slip lines radiating from the centre of the cylinder.

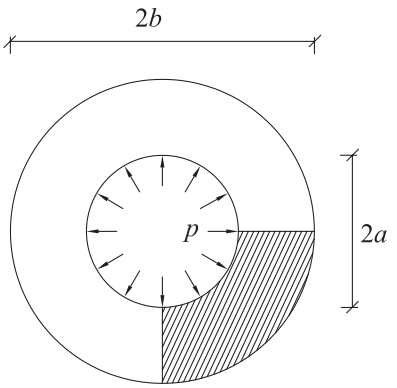

Figure 8. Cylinder expansion problem.

Table VI. Solution statistics, cylinder expansion.

Elem.	Vars.	Equil.	Yield	Err. (%)	Iter.
96	865	800	288	3.54	11
240	2116	1968	720	1.65	15
1200	10 801	9680	3600	0.61	18

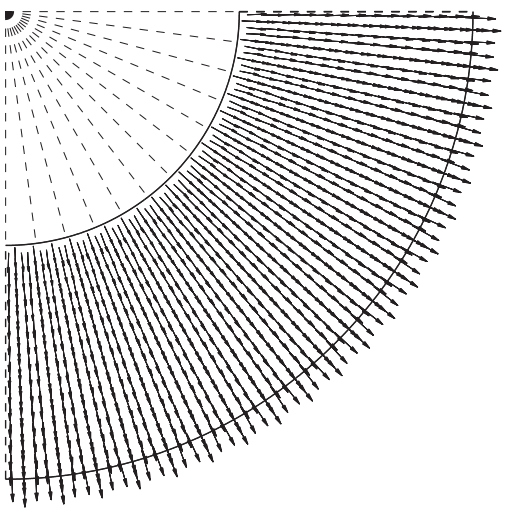

Figure 9. Velocity field, $\phi = 30^\circ$.

To examine the quality of the numerical solution and the behaviour of the optimization algorithm as the angle of friction varies, the finest mesh was used to compute the collapse pressure for different angles of friction. The results are shown of Table VII. As seen, both the error and the iteration counts are more or less constant which indicates that the method should be applicable to the general limit analysis problem governed by the Coulomb criterion. However, further examples are needed in order to confirm this beyond any doubt.

Table VII. Solution statistics for different angles of friction.

ϕ (°)	p/c	Error (%)	Iterations
0	1.3787	0.55	16
10	1.2836	0.58	15
20	1.1574	0.59	17
30	1.0112	0.61	18

5. CONCLUSIONS

A numerical procedure which avoids the need to linearize the yield criteria has been developed for lower bound limit analysis. The optimization algorithm appears to be very efficient with iteration counts being quite insensitive to the problem size.

By using the duality theory in connection with the duality between the upper and lower bound methods, the Lagrange multipliers used in the formulation of the algorithm are interpreted as the displacements and strains at collapse.

The generality and efficiency of the method has been demonstrated by examples of plate and slab structures obeying different non-linear yield criteria.

REFERENCES

1. Damkilde L, Høyer O. An efficient implementation of limit state calculations based on lower-bound solutions. *Computers and Structures* 1993; **49**(6):953–962.
2. Krenk S, Damkilde L, Høyer O. Limit analysis and optimal design of plates with equilibrium elements. *Journal of Engineering Mechanics* (ASCE) 1994; **120**(6):1237–1254.
3. Christiansen E, Andersen KD. Computation of collapse loads with von Mises type yield condition. *International Journal for Numerical Methods in Engineering* 1999; **45**:1185–1202.
4. Lyamin AV, Sloan SW. Upper bound limit analysis using linear finite elements and non-linear programming. In *Finite Elements*: *Techniques and Developments*, Topping BHV (ed.). Civil-Comp Press, Edinburgh, UK, 2000; 131–145.
5. Nash SG, Sofer A. *Linear and Non-linear Programming*. McGraw-Hill: New York, 1996,
6. Krabbenhoft K, Damkilde L. Limit analysis based on lower-bound solutions and non-linear yield criteria. In *Finite Elements*: *Techniques and Developments*, Topping BHV (ed.). Civil-Comp Press, Edinburgh, UK, 2000; 117–129.
7. Poulsen PN, Damkilde L. Limit analysis of reinforced concrete plates subjected to in-plane forces, *International Journal of Solids and Structures* 2000; **37**:6011–6029.
8. Zouain N, Herskovits J, Borges LA, Feijóo RA. An iterative algorithm for limit analysis with non-linear yield functions. *International Journal of Solids and Structures* 1993; **30**(10):1397–1417.
9. Lyamin AV, Three-dimensional lower bound limit analysis using non-linear programming. *Ph.D. Thesis*, University of Newcastle, Newcastle, Australia, July 1999.
10. Fiacco AV, McCormick GP. *Nonlinear Programming*: *Sequential Unconstrained Minimization Techniques*. Wiley: New York, 1968.
11. Lustig IJ, Marsten RE, Shanno DF. Interior point methods for linear programming: computational state of the art, *ORSA Journal on Computing* 1994; **6**(1):1–14.
12. Andersen KD, Christiansen E, Conn AR, Overton ML. An efficient primal-dual interior point method for minimizing a sum of norms. *SIAM Journal on Scientific Computing* 2000; **22**(1):1185–1202.
13. Mehrotra S. On the implementation of a primal-dual interior point method. *SIAM Journal on Optimization* 1992; **2**:575–601.
14. Fox EN. Limit analysis for plates: the exact solution for a clamped square plate of isotropic material obeying the square yield criterion and loaded by uniform pressure. *Philosophical Transactions of the Royal Society* 1974; **A277**:121–155.
15. Yu HS. Expansion of a thick cylinder of soils. *Computers and Geotechnics* 1992; **14**:21–41.

